Author’s Accepted Manuscript

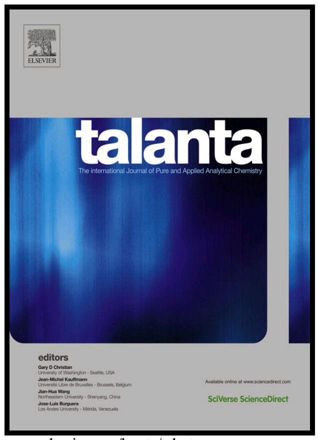

www.elsevier.com/locate/talanta

Optical Sensor based on Hybrid FBG/Titanium Dioxide Coated LPFG for Monitoring Organic Solvents in Edible Oils

Luís Coelho, Diana Viegas, José Luís Santos, José Manuel Marques Martins de Almeida

PII: S0039-9140(15)30440-9
DOI: http://dx.doi.org/10.1016/j.talanta.2015.10.067
Reference: TAL16075

To appear in: *Talanta*

Received date: 28 May 2015
Revised date: 20 October 2015
Accepted date: 24 October 2015

Cite this article as: Luís Coelho, Diana Viegas, José Luís Santos and Jos Manuel Marques Martins de Almeida, Optical Sensor based on Hybri FBG/Titanium Dioxide Coated LPFG for Monitoring Organic Solvents in Edibl Oils, *Talanta,* http://dx.doi.org/10.1016/j.talanta.2015.10.067

Optical Sensor based on Hybrid FBG/Titanium Dioxide Coated LPFG for Monitoring Organic Solvents in Edible Oils

Luís Coelho[a,b], Diana Viegas[c], José Luís Santos[a,b], José Manuel Marques Martins de Almeida[*a,d]

[a]*CAP / INESC TEC - INESC Technology and Science (formerly INESC Porto) and FCUP - Faculty of Sciences, University of Porto*

[b]*Department of Physics, Faculty of Sciences, University of Porto, Rua do Campo Alegre 687, 4169-007 Porto*

[c]*INL – International Iberian Nanotechnology Laboratory, Avenida Mestre José Veiga 4715-330 Braga, Portugal*

[d]*Department of Physics, School of Sciences and Technology, Universidade de Trás-os-Montes e Alto Douro, Apartado 1013, 5001-801 Vila Real, Portugal*

*Corresponding author

email address: jmmma@utad.pt

Abstract

A hybrid optical sensing scheme based on a fiber Bragg grating (FBG) combined with a titanium dioxide coated long period fiber grating (LPFG) for monitoring organic solvents in high refractive index edible oils is reported.

In order to investigate and optimize the sensor performance, two different FBG/LPFG interrogation systems were instigated. The readout of the sensor was implemented using either the wavelength shift of the LPFG resonance dip or the variation in the optical power level of the reflected/transmitted light at the FBG wavelength peak, which in turn depends on the wavelength position of the LPFG resonance.

Hexane concentrations up to 20 % V/V, corresponding to the refractive index range from 1.451 to 1.467, were considered.

For the transmission mode of operation, sensitivities of 1.41 nm / %V/V and 0.11 dB / %V/V, with resolutions of 0.58 %V/V and 0.29 %V/V, were achieved when using the LPFG wavelength shift and the FBG transmitted optical power, respectively.

For the FBG reflection mode of operation, a sensitivity of 0.07 dB / %V/V and a resolution better than 0.16 %V/V were estimated.

Keywords: monitoring contamination of olive oil; organic solvents in edible oils; titanium dioxide coating, long period fiber grating; fiber Bragg grating

1. Introduction

The production of edible oils (EO) is increasing, as reported by the Food and Agriculture Organization (FAO) [1]. Edible oils find application in the food industry as well as in biofuel production, which will drive the EO demand in the next years [2].

Edible oils and fats are virtually omnipresent in food processing, either naturally present in foods or added as ingredients that convey functional properties. Although ingestion levels of oils and fats must be controlled in order to avoid health problems, such as obesity, however, along with proteins and carbohydrates, are one of the three macronutrients and therefore an essential part of a healthy diet [3].

The production of EO consists of two separate processes, extraction and refinement. During extraction, oil is removed from healthy and intact seeds, nuts or fruits and after that refinement alters its appearance, texture, taste, smell or stability to meet consumer expectations [4]. There are three main processes of EO extraction, pressing (using an expeller press), decanter centrifuge and chemical solvent extraction [3]. High quality EO extracted by cold pressing have high tocopherols, sterols, carotenoids, and phospholipids concentrations [5], and a few, such as extra virgin olive oil [6], can be directly consumed unrefined by humans. However, since the oil pomace obtained by pressing still retains 3 to 15 % of residual oil, it is desirable to carry out a more complete extraction with organic solvents.

Modern commercial methods of chemical extraction use volatile purified organic solvents, such as iso-propanol, ethanol, acetone and, especially, the various grades of petroleum benzin, commonly known as petroleum ether or commercial hexane [7]. In fact, a major part of the global EO production in commercial applications derives from chemical extraction processes which have been extensively used in the food industry [8]. These techniques are less expensive, quicker and lead to higher extraction yields [4].

After extraction the oil is separated from the solvent (which is recycled back to the extractor) and then processed using conventional refining techniques such as, degumming, neutralization, washing, drying, bleaching, filtration and deodorization. These processes are intended to remove minor components such as phospholipids, free fatty acids, coloring pigments, proteins and oxidation products [9].

Crude EO contains residual solvents, which raises safety and operational issues during storage and processing. As storage tanks are usually kept at normal pressure, without any inert gas system, the residual solvent may thus accumulate in the vapor phase. The eventual formation of flammable mixtures inside confined volumes may result in explosion in the case of accidental ignition [10]. Recently, several identified accidents involving mixtures of EO with hexane were reported, of which more than half occurred in extraction plants during regular process stages. Two tragic accidents occurred in vegetable oil refineries in Italy in 2006 and in Spain in 2007, due to accidental ignition of flammable mixtures in EO storage tanks [10].

Optical fiber sensors based on long period fiber gratings (LPFG) have been used for sensing of strain, bending and temperature [11], for the detection of organic compounds [12] and as label-free biosensors [13] [14]. They are sensitive to the refractive index (RI) of the medium surrounding the fiber cladding in the grating region, allowing its use as sensing element in chemical and biochemical measurements [15]. The wavelength and amplitude of the attenuation bands depend on the effective RI of the cladding modes, which are a function of the surrounding medium RI.[16, 17].

LPFGs are produced by creating a RI modulation in the fiber core with typical periods in the order of hundreds of micrometers and lengths of a few centimeters [18]. Attenuation bands are generated in the fiber transmission spectrum if the phase matching condition between the fundamental core mode and forward propagating cladding modes is achieved [15].

As the surrounding refractive index (SRI) increases to near cladding refractive index (CRI), there is a shift of the attenuation bands to shorter wavelengths followed by an increase in the transmitted optical power [16, 19]. The highest wavelength sensitivity of the LPGFs occurs for SRI values slightly lower that the CRI [16, 20, 21] and the magnitude of the attenuation band diminishes. However, for SRI higher than the CRI there is very low wavelength sensitivity to SRI variations and a considerable reduction in transmission optical power changes is observed [20]. This disadvantage can be overlapped by coating the bare LPFG with a material that has a RI higher than the cladding [22]. The wavelength shift of the LPFGs depends on the RI and thickness of the film [23], as reported for the case of titanium dioxide (TiO_2) thin film coating [24] and for Langmuir-Blodgett nanolayers [20, 25].

Bare LPFGs were used to detect adulteration of extra virgin olive oil (EVOO) with less expensive sunflower oil [26]. As both oils have refractive indexes higher than the CRI, variation of adulteration level was achieved by monitoring the amplitude changes of the attenuation bands. Furthermore, detection of coconut oil adulterated paraffin oil was attained [27]. In this case, the wavelength sensitivity to SRI variations could be used as sensing mechanism because both oils have refractive indexes smaller than the CRI. It was reported recently the monitoring of thermal deterioration of EVOO (having RI higher than CRI) using an LPFG coated with a TiO_2 thin film [28].

Typically, hybrid FBG / LPFG structures contains two fiber Bragg gratings (FBG) with wavelengths at both sides of attenuation band of the LPFG [29], but operation with a single FBG in one side of the attenuation band is also feasible under certain conditions. Recently, it was reported RI measurements using a LPFG in line with a FBG for temperature compensation [30]. The present work follows a similar configuration, focusing on the development of a hybrid optical sensing structure based on a FBG and a TiO_2 coated LPFG, combination aiming the measurement of concentration of organic solvents in EO. The introduction of the FBG coupled to the LPG generates essentially two major advantages. First it makes the sensing device interrogation easier by measuring the optical power at the FBG wavelength. The second is the possibility of controlling the thermal stability by tracking the wavelength position of the FBG since it is insensitive to the external RI.

The sensing device and its corresponding sensitivity and resolution performance is presented following two different interrogation modes, when operating in reflection and in transmission.

2. Materials and Methods

2.1 Sample Preparation

High quality extra virgin olive oil was acquired in the local market and mixed with *n*-hexane ($CH_3(CH_2)_4CH_3$) (Sigma-Aldrich, Germany), in different proportions, from 1 to 6 % V/V in 1 % V/V steps and from 6 to 20 % V/V in 2 % V/V steps. Afterwards, all samples (each one had a total volume of 25 ml) were mixed, using a vortex mixer (model ZX3, Neu-TEC Group Inc, USA) to ensure total homogenization and were stored in dark glass vials at room temperature (~21 ºC). Measurements were accomplished within ~48 hours.

2.2 Sensor Fabrication

The LPFGs were produced by the electric arc technique as described by Rego et al. [31] in standard single mode fiber (SMF28, Corning, Inc.). The period of the gratings was 396 µm, a value chosen to produce a resonance wavelength at 1.55 µm, matching to the antisymmetric 6th order cladding mode (LP_{16}) according to Ivanov and Rego [32]. The grating attenuation band value was reached with a sensor length of 45±5 mm.

A 30±1.3 nm thick TiO_2 thin film was produced around the grating region by thermal evaporation of pure titanium in a controlled oxygen atmosphere using an electron beam evaporator (Auto 306, Edwards Ltd, U.K.). The details of the manufacturing process were presented recently [24]. The RI of a Ti_2O thin film deposited on a silicon substrate was estimated with an AutoSE ellipsometer (HORIBA Scientific, U.S.A.) in the 500-800 nm range. A nonlinear fit was applied to the set of 218 experimental data points using the Sellmeier equation in order to estimate the real RI component at 1550 nm.

The FBGs were written in hydrogen loaded standard single-mode telecommunication fiber (SMF28, Corning Inc.) using the phase mask technique [33] and had wavelength peak positions at 1539.91 and 1554.54 nm at room temperature. The two gratings were then fusion spliced to the LPFG to create the fiber sensor structures illustrated in Fig. 1.

2.3 Experimental Setup

The coated LPFG was characterized with an optical spectrum analyzer (OSA) (ANDO, model AQ 6315B), following the procedure described elsewhere [24], using a set of RI calibrated oils (Cargille-Sacher Laboratories Inc., NJ. U.S.A.) in the RI range from 1.300 to 1.640.

Prior to the oil characterization using the FBG / LPFG sensors, the RI of the samples was measured at room temperature (26±1 ºC) using an Abbe refractometer (A. Kruss, Optronic, Germany) with a RI resolution of 2.5×10^{-4}.

Two similar FBG / LPFG sensors (labelled SMF 1 and SMF 2 in Fig.1 a) were used simultaneously to characterize the refractive index variation of the oil samples, as illustrated in the setup of Fig. 1 b).

Sensor SMF 1 was intended for interrogation in transmission mode only. For that purpose it was used a homemade broadband source (BBS) and the OSA, with a resolution of 0.2 nm and a sampling rate of 1 spectrum per minute, from 1500 to 1630 nm.

Sensor SMF 2 was planned to be used as a sensing tip interrogated in reflection mode, however it was also characterized in transmission mode, as shown in Fig. 1 a). The spectra were measured using a computer controlled unit specifically designed to interrogate FBGs but also capable to be used as OSA (BraggMETER FS2200 SA, FiberSensing, Porto, Portugal), with a resolution of 1 pm at a sampling rate of 1 spectrum per second, from 1500 to 1600 nm.

The setup shown in Fig. 1 b) is constituted by a homemade flow cell made of Poly (methyl methacrylate) (PMMA) with two identical channels and six openings, four of them used to pass the fibers containing sensors and the other two to fill and to drain liquid samples. Both sensors were inserted in the cell and the FBG / LPFG structures were aligned with the center of the channels. To avoid fiber-bending interference on the sensing response the ends of the fibers were clamped by pressing and holding the base of the flow cell against its upper half.

After each measurement the flow cell was flushed with 20 ml of ethanol (Merk Millipore, Germany) and dried with filtered air to avoid contamination to the next oil sample. Then the spectrum of each sensor was monitored to ensure that the resonance dip has returned to its original spectral position.

3. Results and Discussion

The wavelength shift normalized to the initial RI state (n = 1) as a function of the SRI, from 1.300 to 1.640, was reported in [28] for the LP_{16} mode for a bare LPFG and for a 30 nm TiO_2 coated LPFG. For SRI higher than the CRI the bare LPFG presents virtually no wavelength shift sensitivity whereas the coated LPFG presents a high sensitivity. For instance, in the 1.46 to 1.48 RI range, characteristic of EO, the measured average sensitivity is about ~800 nm/RIU [28].

The RI of the pure olive oil was 1.46650±0.00025 and as the hexane concentration increases (whose RI is 1.3735), the RI of the mixture diminishes, as illustrated in Fig. 2. From a linear fit to the data with a correlation coefficient (R^2) of 0.998, a rate of 0.076 RIU / %V/V was calculated.

It follows that the concentration of hexane in olive oil can be monitored by measuring the RI of the mixture, which in turn can be evaluated by measuring the specific spectral characteristics of the LPFG resonance band.

3.1 OSA Spectral Data

Analysis of the LPFG 1 wavelength shift

For the SMF 1 sensor, Fig. 3 shows the spectral behavior of the LP_{16} band characteristic of the LPFG 1, together with the FBG 1 dip at 1539.91 nm, for increasing hexane concentration. It is also shown the LPFG spectra taken with air and with hexane as external medium. The spectral data was subjected to a fast Fourier transform (FFT) smoothing filter to reduce the noise due to the low power level of the light that reaches the OSA. As the corresponding RI decreases, the LP_{16} band exhibits a notorious redshift.

For achieving the minimum of the LPFG dip in terms of wavelength and optical power care must be taken because the attenuation bands are in most cases asymmetric. However, the lower part of the bands is with reasonable accuracy a symmetric curve which can be fitted by a symmetric function. To perform this analysis the minimum optical power of the band was evaluated and then considering only the points 15% above this minimum, a Gaussian function was fitted and all the parameters were extracted, such as the wavelength position and the minimum optical power.

The experimental wavelength shift of the resonance dip is shown in Fig. 4 as a function of either the hexane concentration or the resulting RI of the mixture. For hexane concentration up to 16 % V/V the average sensitivity of 1.41 nm / % V/V (or 1881.2 nm/RIU) was calculated.

The temperature around the flow cell was measured by a digital thermocouple (Model DVM1322, Velleman, Belgium) and found to increase ~1.5 ºC during the measurements. It is well known that optical fiber gratings are sensitive to temperature variations [34]. The temperature sensitivity of the LP_{16} band of coated TiO_2 LPFG sensor was measured from 30 to 85 ºC. As shown in the inset of Fig 2, a linear fit was established, from which a sensitivity of 113pm / ºC was measured for this specific mode. Therefore, for a temperature increase of 1.5 ºC, the highest expected error in the determination of the wavelength of the LP_{16} dip is lower than 0.2 nm.

The spectral resolution, R, can be estimated considering the values obtained from two measurement linked with two different values of the external RI, obtained from the following expression [35]:

$$R = \frac{\sigma}{S_{RI}} = \frac{\delta n}{\delta \lambda} \sigma$$

where the δn is the RI difference, S_{RI} is the sensitivity to RI variations, $\delta \lambda$ is the difference in the wavelength resonant dip and σ is the noise induced highest standard deviation associated with the sensor output variation coupled to a step variation of the external RI.. Fig. 5 shows data concerning two of these steps $\left(\delta n_1 = 0.00200, \delta n_1 = 0.00225\right)$. From the two steps, shown in Fig. 5 a spectral resolution better than 0.58 %V/V (or 5.8x10^{-4} RIU) was calculated. To check the stability/repeatability of the process, the same samples solutions were used to obtain several acquisitions, confirming the effectiveness of this sensing structure.

Analysis of the FBG 1 transmission

Increasing the hexane concentration leads to a RI reduction and to a redshift of the LP_{16} mode, which in turn conducts to an increment of the transmitted optical power in the left wing of the LPFG 1 resonance band. Also, it leads to an almost symmetrical transmission diminution on the right wing of the resonance band (see Fig. 3). Therefore, the spectral signature at 1539.91 nm of the FBG 1 (located on the left side of the band dip) associated with the SMF1 sensor can be used to monitor the transmitted optical power through the sensor. Figure 6 displays the variation of the optical power transmitted through the FBG 1 due to the continuous fading of the low wavelength region of the resonance band when the hexane concentration increases. The continuous line in the graph is a linear fit to the experimental points (excluding two outlier samples corresponding to 18 and 20 %V/V), characterized by a R^2 value of 0.992. For hexane concentrations up to 16 %V/V the sensitivity is 0.11 dB / %V/V (or 170.8 dB/RIU).

Following the procedure outlined above, the resolution of this measurement methodology can be calculated considering the values obtained from two measurements linked with two different values of the external RI:

$$R = \frac{\sigma}{S_{RI}} = \frac{\delta n}{\delta P}\sigma$$

where δP is the difference in the output power of the FBG 1. From the two steps, shown in Fig. 7, a resolution of 0.29 %V/V (or 2.1x10^{-4} RIU) was estimated.

3.2 Analysis of the data from the BraggMeter

For the SMF 2 sensor, Fig. 8 shows the spectral behavior of the LP_{16} band of the LPFG 2 after signal to noise improvement using the same FFT smoothing filter. Similar comments can be applied to this grating, namely, the wavelength sensitivity and spectral resolution which are of the same order of magnitude as stated above for the LPFG 1 analyzed in transmission mode.

Analysis of the FBG 2 in reflection and transmission modes

Sensor SMF 2 was planned to be a sensing tip. Using the concept applied to SMF 1 sensor the continuous vanishing of the LP_{16} band with increasing hexane concentration leads to an increase of the optical power reaching the FBG 2. The spectral feature at 1554.54 nm, characteristic of the FBG 2 is shown in Fig. 8. Part of the radiation transmitted double crosses the LPFG 2 upon reflection in the FGB 2, being then detected by the interrogation unit (BraggMETER, FS2200 SA). In addition, as described above, FBG 2 can be used to monitor the transmitted optical power through the LPFG 2.

Figure 9 displays the magnitude of the measured optical power shift due to signal reflection on FBG 2 and due to the signal transmitted through it. The continuous lines are linear fits to the experimental points (excluding two samples at 14 and 16 % V/V). For hexane concentrations up to 12 % V/V the sensitivity in reflection is 0.07 dB / % V/V and in transmission is higher, 0.12 dB / % V/V. Both fits are characterized by R^2 higher than 0.98.

Figure 10 illustrates the time evolution of the sensor readout, both in reflection and in transmission, from which the calculated resolution was higher for reflection, 0.16 %V/V (or 1.4×10^{-4} RIU) than for transmission, 0.31 %V/V (or 2.3×10^{-4} RIU).

Table 1 resumes the sensitivities and resolution for both sensors and measurement techniques.

According to the inset of Fig. 2 the FBGs used in the present work have a temperature sensitivity of ~11 pm/ºC which is in agreement with the literature for the standard communication optical fiber (~10pm/ºC) [36]. As can be observed in the right axis of Fig. 9, a wavelength shift of 16.5 pm of the FBG 2 occurred during the experiment, from which a temperature variation of 1.5 ºC within the flow cell was calculated, a value compatible with the temperature variation just outside the cell.

While the LPFG sensors are sensitive to both SRI and temperature variation, FBG are SRI insensitive. The proposed hybrid configuration allows correction of the LPFG wavelength shift due to random temperature drifts, which may occur in crude EO storage. Moreover, in temperature dependent laboratorial or industrial processes, such as in EO chemical extraction, accurate monitoring of hexane concentration would require wavelength shift correction.

4. Conclusions

An optical sensing scheme based on hybrid FBG/LPFG coated with titanium dioxide for monitoring organic solvents in edible oils is reported.

Despite the advantages of a probe tip geometry and of the easiest of the sensor interrogation in reflection mode, the study showed that the highest sensitivity was obtained in transmission mode. The resolution, however is lower in transmission mode as compared with reflection mode. SMF 1 and SMF 2 sensors present sensitivities between 0.11 and 0.12 dB / %V/V when interrogated in transmission mode, a value higher than the value of 0.07 dB / %V/V, achieved for the FBG readout in reflection mode. However, the lowest resolution is attained in reflection mode (0.16 %V/V).

The use of the LPFG wavelength sensitivity of 1881.2 nm / RIU together with a commercial available OSA with 0.1 nm resolution, would allow the implementation of a sensing system with resolutions of ~10^{-5} RIU or ~0.08 %V/V.

In conclusion, the hybrid FBG/titanium dioxide coated LPFG sensing structure may find application in the monitoring of high refractive index liquids such as hexane or other organic solvents in storage tanks and processing reactors in EO extraction and refining plants.

Acknowledgements

This work was partially financed by the FCT – Fundação para a Ciência e a Tecnologia (Portuguese Foundation for Science and Technology) within project UID/EEA/50014/2013.

L. Coelho acknowledges the support from FCT grant SFRH/BD/78149/2011.

References

[1] F.a.A. Organization, FAO 2009. Information available at the website http://www.fao.org, 2009.

[2] OECD-FAO, Agricultural Outlook 2006–2015, Paris, 2006.

[3] W.H.R.J.C.G. Hamm, Edible Oil Processing, 2nd ed., Wiley-Blackwell2013.

[4] R.D.F. O'Brien, W.E. ; Wan, P.J. , Introduction to Fats and Oils Technology, 2nd ed., AOCS Press, Champaign, 2000.

[5] A. Obiedzinska, B. Waszkiewicz-Robak, COLD PRESSED OILS AS FUNCTIONAL FOOD, Zywnosc-Nauka Technologia Jakosc, 19 (2012) 27-44.

[6] D. Boskou, Olive Oil: Chemistry and Technology 2nd ed., AOCS Press, Champaign, Illinois, 2006.

[7] N.T. Dunford, M.Q. Zhang, Pressurized solvent extraction of wheat germ oil, Food Research International, 36 (2003) 905-909.

[8] F. Shahidi, Edible Oil and Fat Products: Edible Oils. In: Bailey's industrial oil and fat products, Sixth ed. ed., Wiley & Sons, New York, 2005.

[9] G.F.D.H.J.L.D. A.J., The Lipid Handbook, 3rd ed., CRC Press, Taylor & Francis, London, 2007.

[10] G. Landucci, B. Nucci, L. Pelagagge, C. Nicolella, Hazard assessment of edible oil refining: Formation of flammable mixtures in storage tanks, Journal of Food Engineering, 105 (2011) 105-111.

[11] B.H. Lee, Y.H. Kim, K.S. Park, J.B. Eom, M.J. Kim, B.S. Rho, H.Y. Choi, Interferometric fiber optic sensors, Sensors, 12 (2012) 2467-2486.

[12] T. Allsop, L. Zhang, I. Bennion, Detection of organic aromatic compounds in paraffin by a long-period fiber grating optical sensor with optimized sensitivity, Optics Communications, 191 (2001) 181-190.

[13] P. Pilla, V. Malachovská, A. Borriello, A. Buosciolo, M. Giordano, L. Ambrosio, A. Cutolo, A. Cusano, Transition mode long period grating biosensor with functional multilayer coatings, Optics express, 19 (2011) 512-526.

[14] F. Baldini, F. Chiavaioli, A. Giannetti, M. Brenci, C. Trono, Label-free biosensor based on long period grating, 2013, pp. 857217-857217-857216.

[15] S. James, R. Tatam, Optical fibre long-period grating sensors: Characteristics and application, Measurement Science & Technology, 14 (2003) R49-R61.

[16] H. Patrick, A. Kersey, F. Bucholtz, Analysis of the response of long period fiber gratings to external index of refraction, J. Lightwave Technol., 16 (1998) 1606-1612.

[17] X. Shu, L. Zhang, I. Bennion, Sensitivity characteristics of long-period fiber gratings, J. Lightwave Technol., 20 (2002) 255-266.

[18] A. Vengsarkar, P. Lemaire, J. Judkins, V. Bhatia, T. Erdogan, J. Sipe, Long-period fiber gratings as band-rejection filters, J. Lightwave Technol., 14 (1996) 58-65.

[19] G. Rego, A review of refractometric sensors based on long period fibre gratings, TheScientificWorldJournal, 2013 (2013) 913418.

[20] E. Simoes, I. Abe, J. Oliveira, O. Frazao, P. Caldas, J. Pinto, Characterization of optical fiber long period grating refractometer with nanocoating, Sensors and Actuators B-Chemical, 153 (2011) 335-339.

[21] S. Khaliq, S. James, R. Tatam, Enhanced sensitivity fibre optic long period grating temperature sensor, Measurement Science & Technology, 13 (2002) 792-795.

[22] I. Del Villar, I. Matias, F. Arregui, P. Lalanne, Optimization of sensitivity in long period fiber gratings with overlay deposition, Optics Express, 13 (2005) 56-69.

[23] P. Pilla, C. Trono, F. Baldini, F. Chiavaioli, M. Giordano, A. Cusano, Giant sensitivity of long period gratings in transition mode near the dispersion turning point: an integrated design approach, Opt. Lett., 37 (2012) 4152-4154.

[24] L. Coelho, D. Viegas, J.L. Santos, J.M.M.M.d. Almeida, Enhanced refractive index sensing characteristics of optical fibre long period grating coated with titanium dioxide thin films, Sensors and Actuators B: Chemical, 202 (2014) 929-934.

[25] N. Rees, S. James, R. Tatam, G. Ashwell, Optical fiber long-period gratings with Langmuir-Blodgett thin-film overlays, Opt. Lett., 27 (2002) 686-688.

[26] T.M. Libish, M.C. Bobby, J. Linesh, S. Mathew, C. Pradeep, V.P.N. Nampoori, P. Biswas, S. Bandyopadhyay, K. Dasgupta, P. Radhakrishnan, Detection of adulteration in virgin olive oil using a fiber optic long period grating based sensor, Laser Physics, 23 (2013) 045112.

[27] T.M. Libish, J. Linesh, M.C. Bobby, P. Biswas, S. Bandyopadhyay, K. Dasgupta, P. Radhakrishnan, Detection and analysis of paraffin oil adulteration in coconut oil using fiber optic long period grating sensor, Optik - International Journal for Light and Electron Optics, 122 (2011) 1939-1942.

[28] L. Coelho, D. Viegas, J.L. Santos, J.M.M.M. de Almeida, Detection of extra virgin olive oil thermal deterioration using a long period fibre grating sensor coated with titanium dioxide, Food and Bioprocess Technology: An International Journal, DOI 10.1007/s1194701514899(2015).

[29] H. Patrick, G. Williams, A. Kersey, J. Pedrazzani, A. Vengsarkar, Hybrid fiber Bragg grating/long period fiber grating sensor for strain/temperature discrimination, Photonics Technology Letters, IEEE, 8 (1996) 1223-1225.

[30] C. Berrettoni, C. Trono, V. Vignoli, F. Baldini, Fibre Tip Sensor with Embedded FBG-LPG for Temperature and Refractive Index Determination by means of the Simple Measurement of the FBG Characteristics, Journal of Sensors, 2015 (2015) 8.

[31] G. Rego, J. Santos, H. Salgado, Refractive index measurement with long-period gratings arc-induced in pure-silica-core fibres, Optics Communications, 259 (2006) 598-602.

[32] O. Ivanov, G. Rego, Origin of coupling to antisymmetric modes in arc-induced long-period fiber gratings, Optics express, 15 (2007) 13936-13941.

[33] K.O. Hill, B. Malo, F. Bilodeau, D.C. Johnson, J. Albert, Bragg gratings fabricated in monomode photosensitive optical fiber by UV exposure through a phase mask, Appl. Phys. Lett., 62 (1993) 1035-1037.

[34] A. Singh, D. Engles, A. Sharma, M. Singh, Temperature sensitivity of long period fiber grating in SMF-28 fiber, Optik-International Journal for Light and Electron Optics, 125 (2014) 457-460.

[35] N. Díaz-Herrera, A. González-Cano, D. Viegas, J.L. Santos, M.-C. Navarrete, Refractive index sensing of aqueous media based on plasmonic resonance in tapered optical fibres operating in the 1.5µm region, Sensors and Actuators B: Chemical, 146 (2010) 195-198.

[36] B. Sutapun, M. Tabib-Azar, A. Kazemi, Pd-coated elastooptic fiber optic Bragg grating sensors for multiplexed hydrogen sensing, Sensors and Actuators B-Chemical, 60 (1999) 27-34.

Figure captions

Figure 1. a) Scheme of the measurement setup including: broadband source - BBS, optical spectrum analyzer - OSA, sensors - SMF1/SMF2, FBGs interrogation unit/OSA – Model FS2200

b) PMMA flow cell with two channels and six openings, four to pass the fibers and two to fill and drain liquid samples.

Figure 2. Refractive index of the samples for hexane concentration from 0 to 20 % V/V. Inset: temperature sensitivities of both LPFG and FBG from 30 to 80 ºC.

Figure 3. Spectral features of the LP_{16} band characteristic of the LPFG 1 (SMF 1 sensor), for air as external medium, pure hexane, olive oil and for mixtures with olive oil and various hexane concentrations.

Figure 4. Wavelength shift of the LP_{16} band dip of the LPFG 1 (SMF 1 sensor) as a function of the hexane concentration (and of the refractive index). The continuous line is a linear fitting up to 16 % V/V.

Figure 5. Wavelength variation of the dip from LPFG 1 (SMF 1 sensor) when the surrounding medium undertakes step variations of hexane concentration (or refractive index).

Figure 6. Dependence of the transmitted optical power shift of the FBG 1 (SMF 1 sensor) on the hexane concentration (and on the refractive index). The continuous line is a linear fitting up to 16 % V/V.

Figure 7. Variation of the optical power transmitted by FBG 1 (SMF 1 sensor) when the surrounding medium undertakes step variations of hexane concentration (or refractive index).

Figure 8. Spectral features of the LP_{16} band characteristic of the LPFG 2 (SMF 2 sensor), for air as external medium, pure water, ethanol, hexane, olive oil and for mixtures with olive oil and various hexane concentrations.

Figure 9. Left axis: dependence of the transmitted and of the reflected optical power shift of the FBG 2 (SMF 2 sensor) on the hexane concentration (and on the refractive index). Right axis: FBG 2 wavelength shift during the measurements.

Figure 10. Variation of the optical power transmitted and reflected by FBG 2 (SMF 2 sensor) when the surrounding medium undertakes step variations of hexane concentration (or refractive index).

Table captions

Table 1. Summary of the sensitivity and resolution of SMF 1 and SMF 2 sensors interrogated in both modes, transmission and reflection.

Graphical abstract

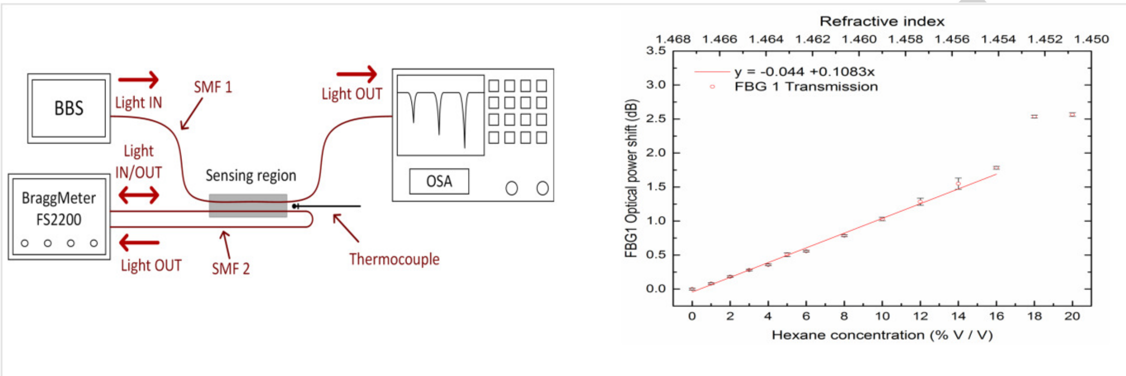

Highlights

● Refractive index sensor based on hybrid FBG/TiO2 coated LPFG demonstrated.

● Suitability of the sensor for monitoring organic solvents in edible oils is reported.

● Minimum measurable hexane concentration in olive oil is 0.08 %V/V.

● Wavelength sensitivity of 1881 nm/RIU was achieved in the range 1.451 to 1.467

● Refractive index resolution of $1.4x10^{-4}$ was achieved in the range 1.451 to 1.467.

Table 1

	SMF1			SMF2		
	Wavelength shift		**Optical power**	**Optical power**		**Units**
Sensitivity	1.41	**nm / %V/V**	0.11	0.12	0.07	**dB / %V/V**
	1881.2	**nm / RIU**	170.8	160.5	89.7	**dB / RIU**
Resolution	0.58		0.29	0.31	0.16	**%V/V**
	$5.8x10^{-4}$		$2.1x10^{-4}$	$2.3x10^{-4}$	$1.4x10^{-4}$	**RIU**
	Transmitted			**Transmitted**	**Reflected**	

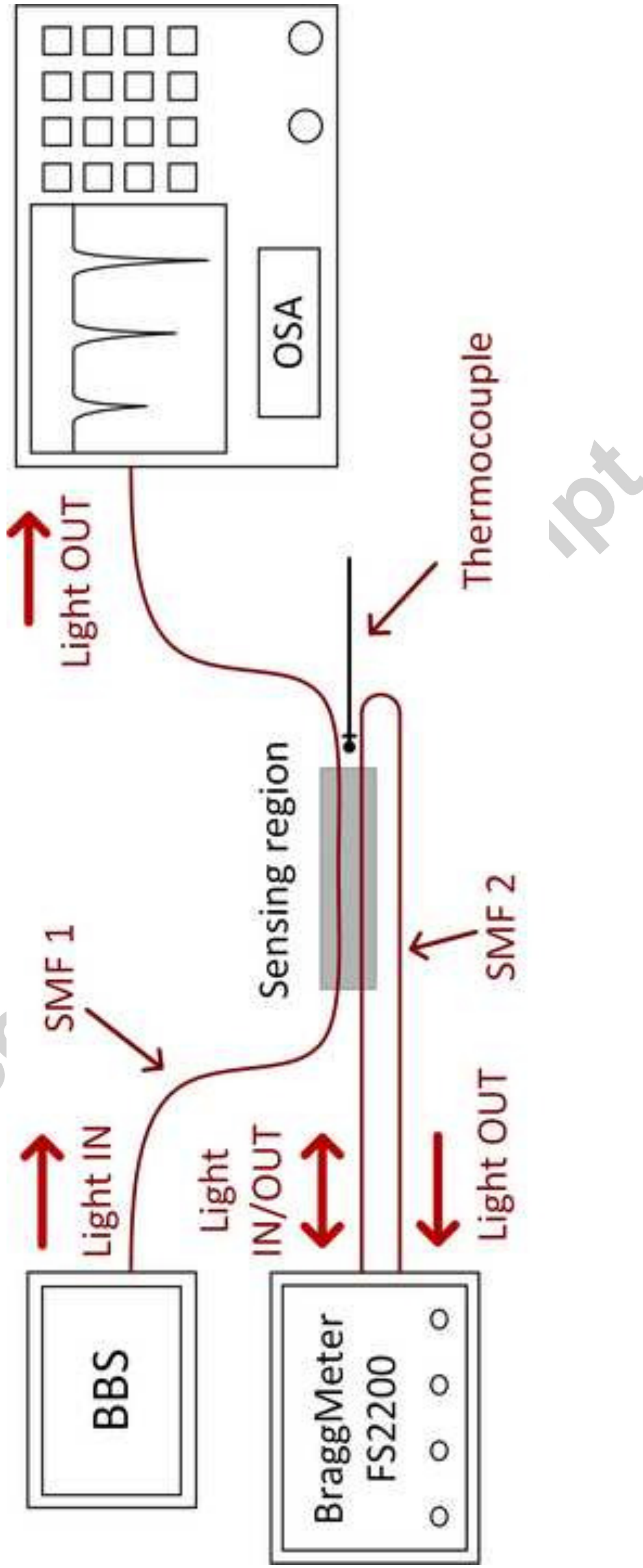
OSA
Light OUT
Thermocouple
Sensing region
SMF 1
SMF 2
Light IN
Light IN/OUT
Light OUT
BBS
BraggMeter FS2200

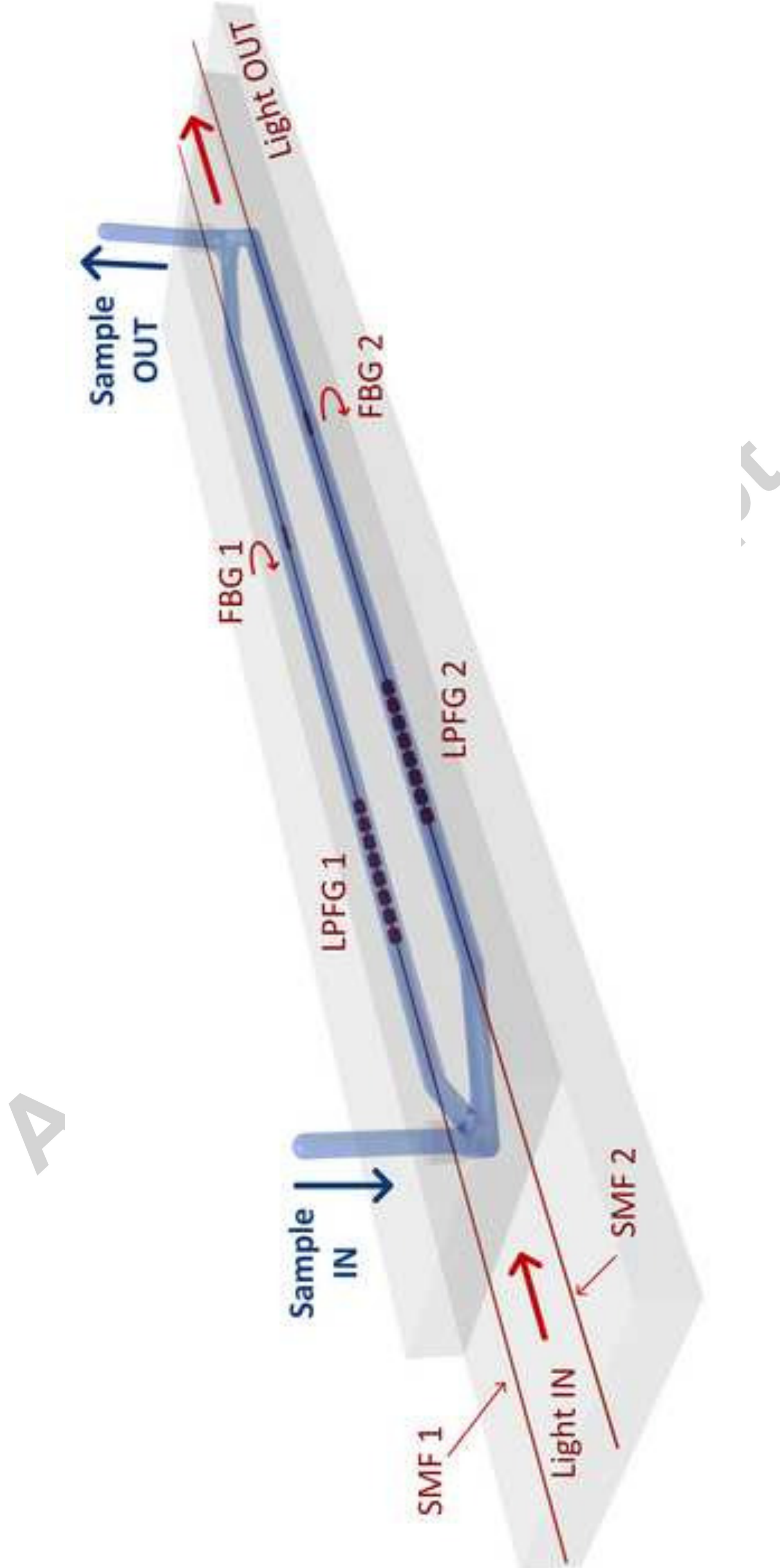
Light OUT
Sample OUT
FBG 2
FBG 1
LPFG 2
LPFG 1
Sample IN
SMF 2
SMF 1
Light IN

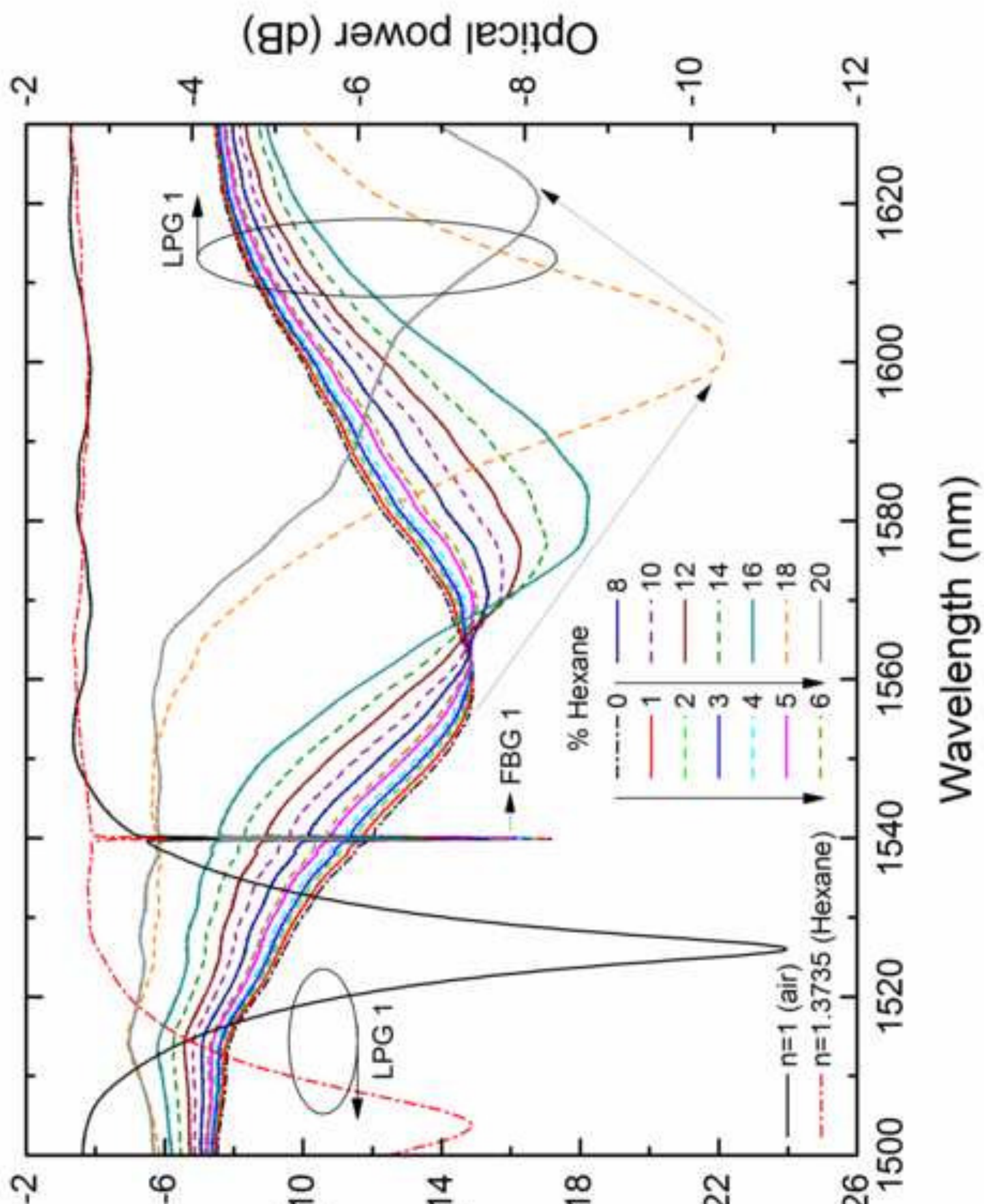
Wavelength (nm)
Optical power (dB)
Optical power (dB)
LPG 1
LPG 1
FBG 1
% Hexane
0
1
2
3
4
5
6
8
10
12
14
16
18
20
n=1 (air)
n=1.3735 (Hexane)

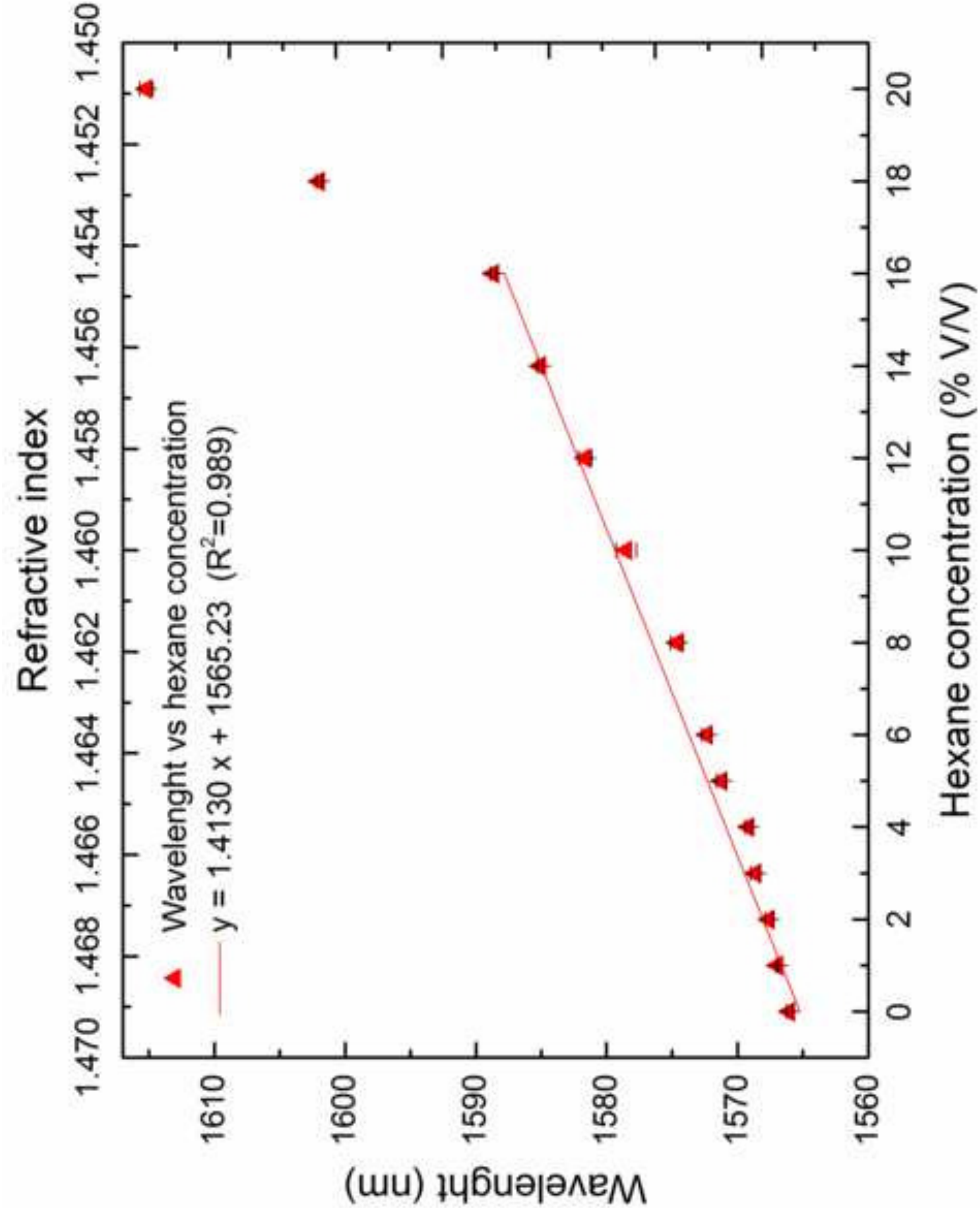

Refractive index
1.470
1.468
1.466
1.464
1.462
1.460
1.458
1.456
1.454
1.452
1.450
Wavelenght vs hexane concentration
y = 1.4130 x + 1565.23 (R^2=0.989)
Wavelenght (nm)
1610
1600
1590
1580
1570
1560
0
2
4
6
8
10
12
14
16
18
20
Hexane concentration (% V/V)

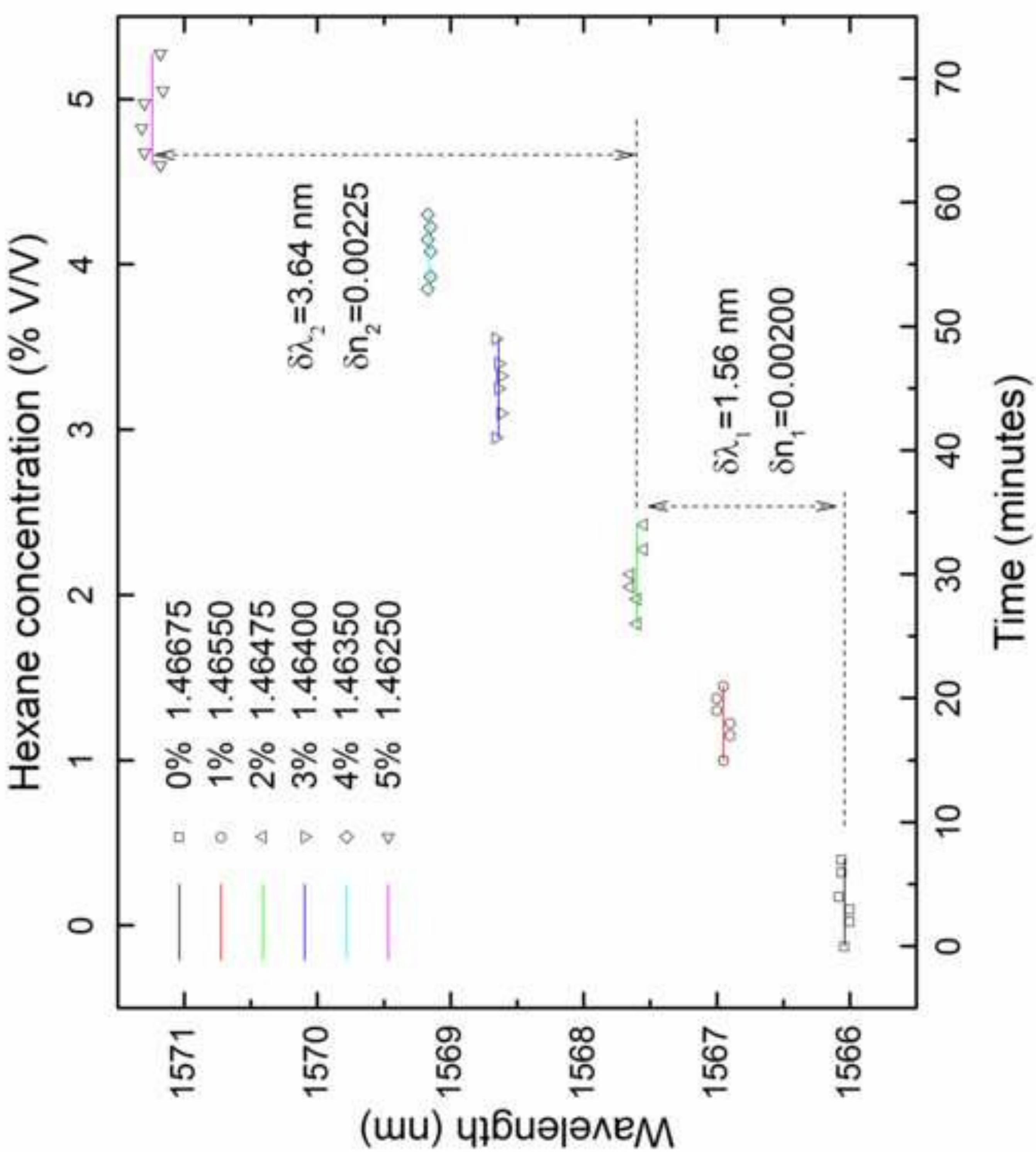

Hexane concentration (% V/V)
0 1 2 3 4 5
0% 1.46675
1% 1.46550
2% 1.46475
3% 1.46400
4% 1.46350
5% 1.46250
δλ2=3.64 nm
δn2=0.00225
δλ1=1.56 nm
δn1=0.00200
Wavelength (nm)
1571 1570 1569 1568 1567 1566
Time (minutes)
0 10 20 30 40 50 60 70

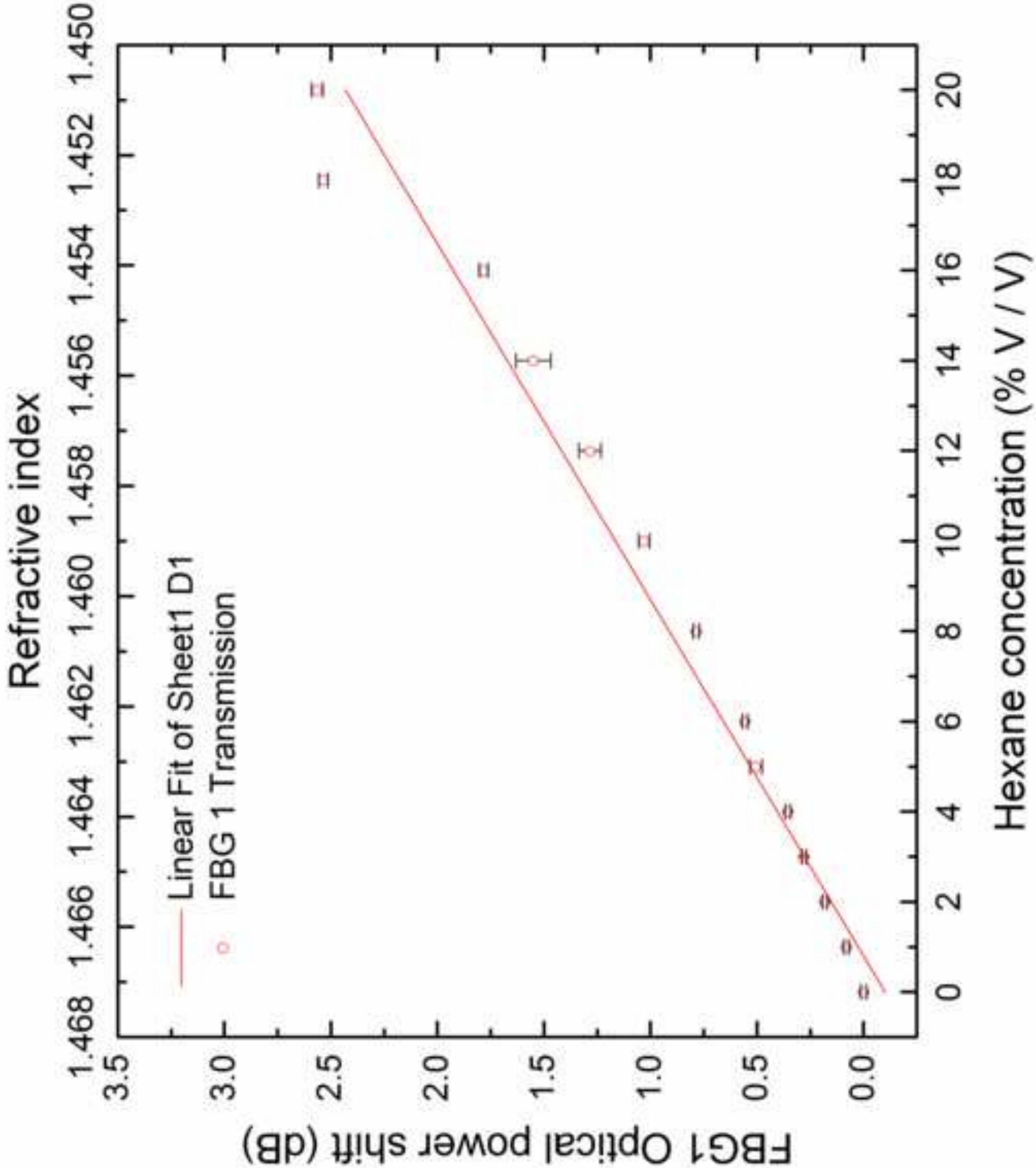
Refractive index
Hexane concentration (% V / V)
FBG1 Optical power shift (dB)
Linear Fit of Sheet1 D1
FBG 1 Transmission
1.468
1.466
1.464
1.462
1.460
1.458
1.456
1.454
1.452
1.450
0
2
4
6
8
10
12
14
16
18
20
0.0
0.5
1.0
1.5
2.0
2.5
3.0
3.5

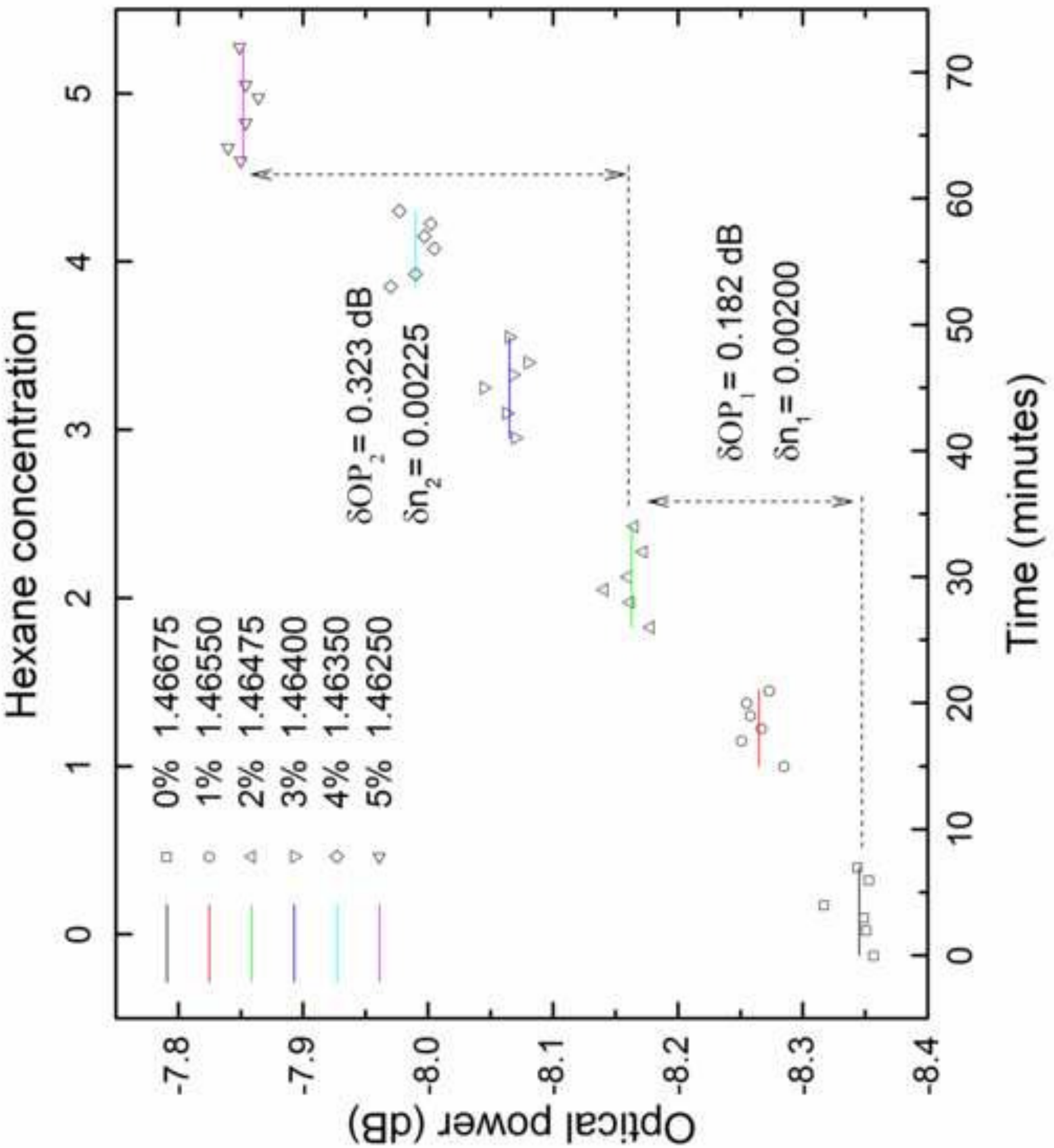

Hexane concentration
0
1
2
3
4
5
0% 1.46675
1% 1.46550
2% 1.46475
3% 1.46400
4% 1.46350
5% 1.46250
δOP2 = 0.323 dB
δn2 = 0.00225
δOP1 = 0.182 dB
δn1 = 0.00200
Optical power (dB)
-7.8
-7.9
-8.0
-8.1
-8.2
-8.3
-8.4
Time (minutes)
0
10
20
30
40
50
60
70

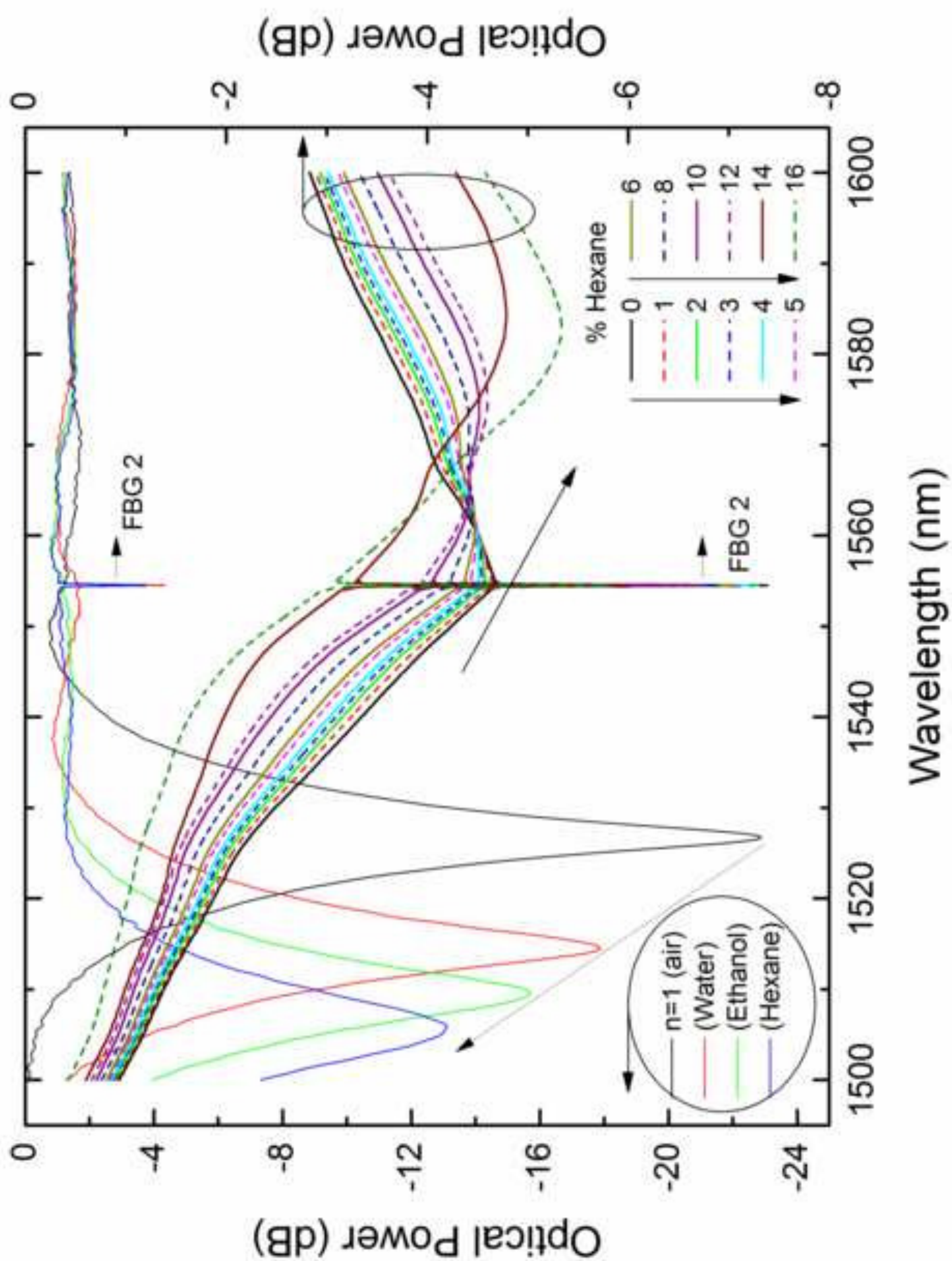
Optical Power (dB)
Optical Power (dB)
Wavelength (nm)
FBG 2
FBG 2
% Hexane
0
1
2
3
4
5
6
8
10
12
14
16
n=1 (air)
(Water)
(Ethanol)
(Hexane)

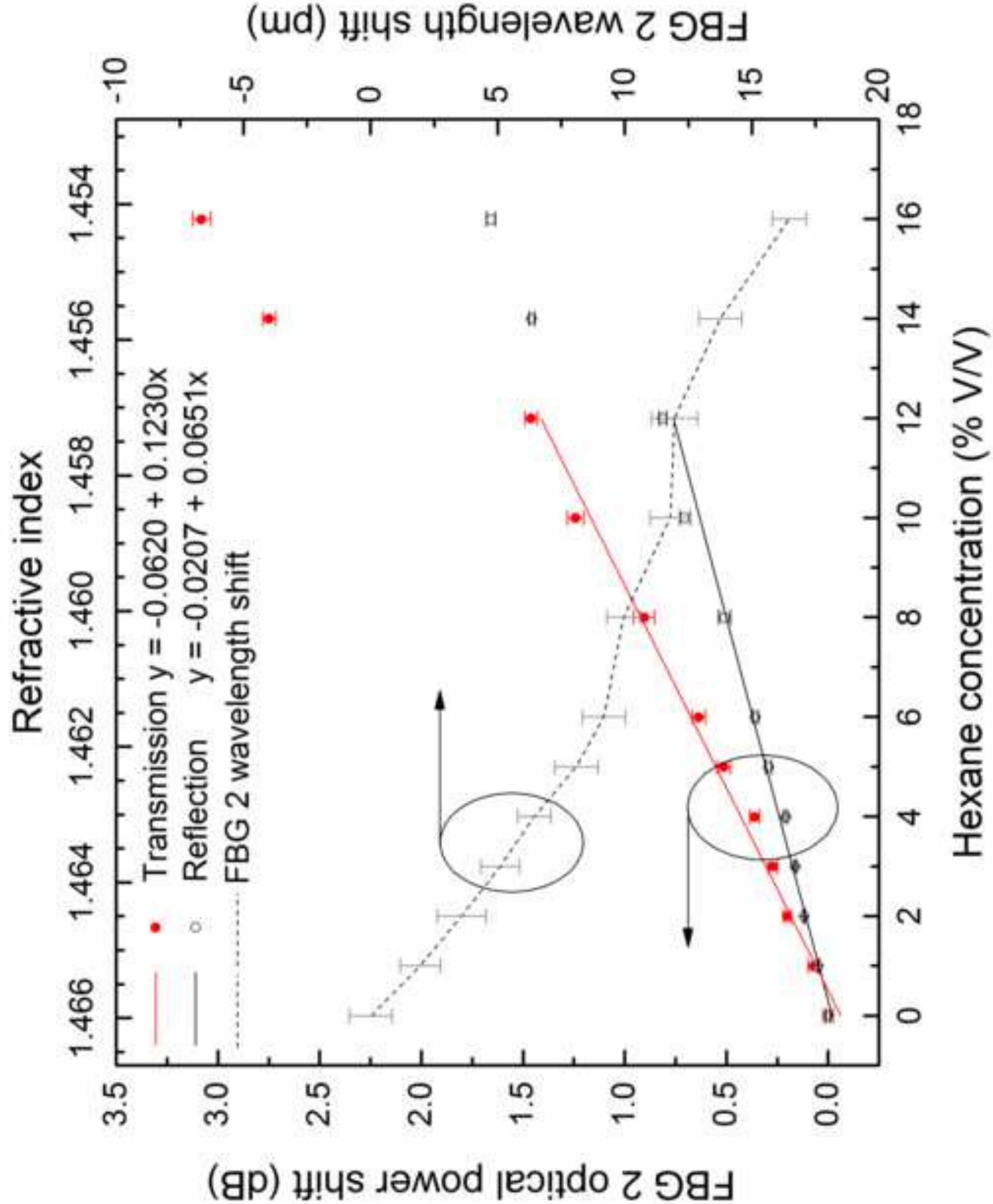
Refractive index
1.466
1.464
1.462
1.460
1.458
1.456
1.454
FBG 2 wavelength shift (pm)
-10
-5
0
5
10
15
20
FBG 2 optical power shift (dB)
3.5
3.0
2.5
2.0
1.5
1.0
0.5
0.0
Hexane concentration (% V/V)
0
2
4
6
8
10
12
14
16
18
Transmission y = -0.0620 + 0.1230x
Reflection y = -0.0207 + 0.0651x
FBG 2 wavelength shift

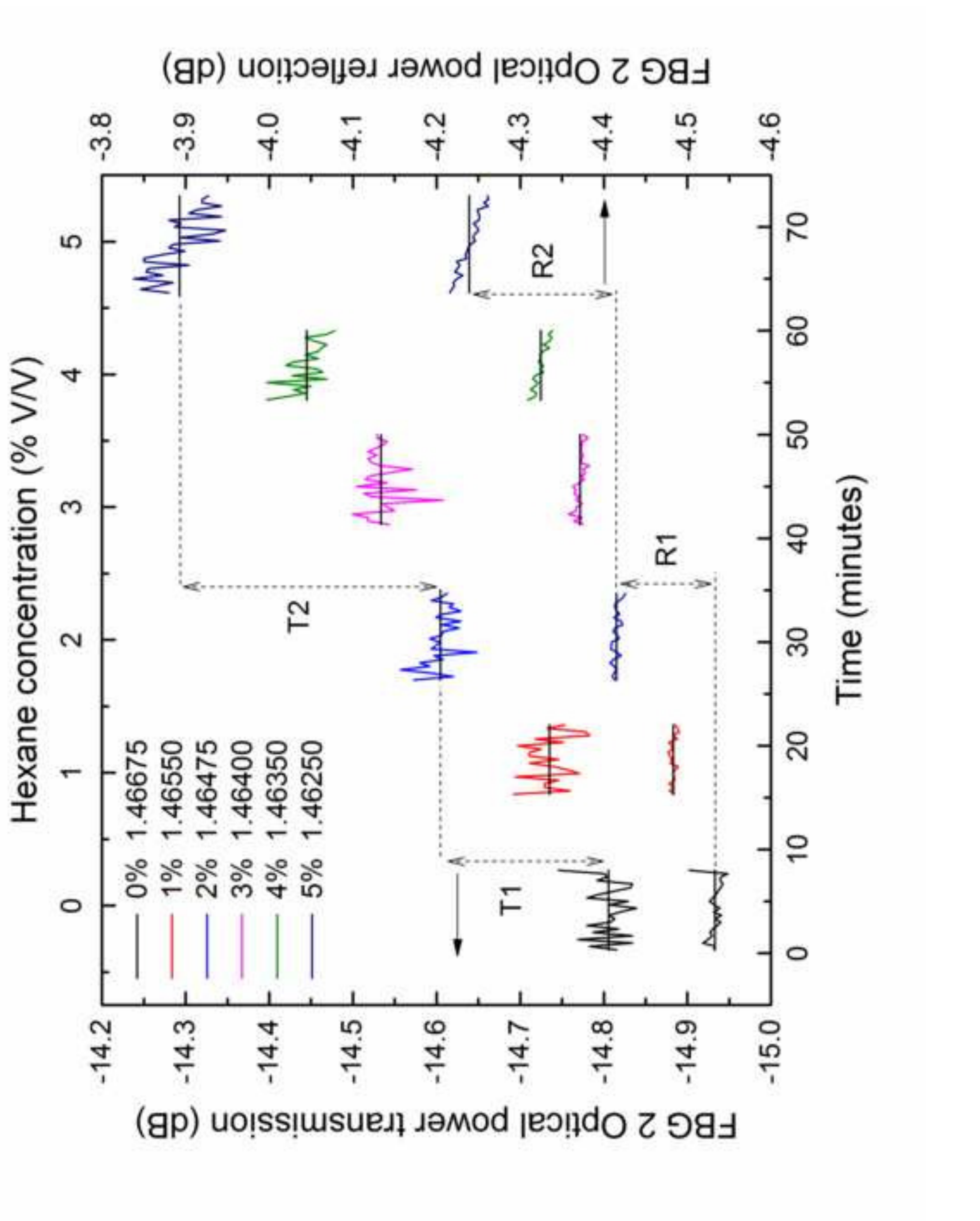

Hexane concentration (% V/V)
FBG 2 Optical power reflection (dB)
FBG 2 Optical power transmission (dB)
Time (minutes)
0
1
2
3
4
5
-3.8
-3.9
-4.0
-4.1
-4.2
-4.3
-4.4
-4.5
-4.6
-14.2
-14.3
-14.4
-14.5
-14.6
-14.7
-14.8
-14.9
-15.0
0
10
20
30
40
50
60
70
0% 1.46675
1% 1.46550
2% 1.46475
3% 1.46400
4% 1.46350
5% 1.46250
T1
T2
R1
R2

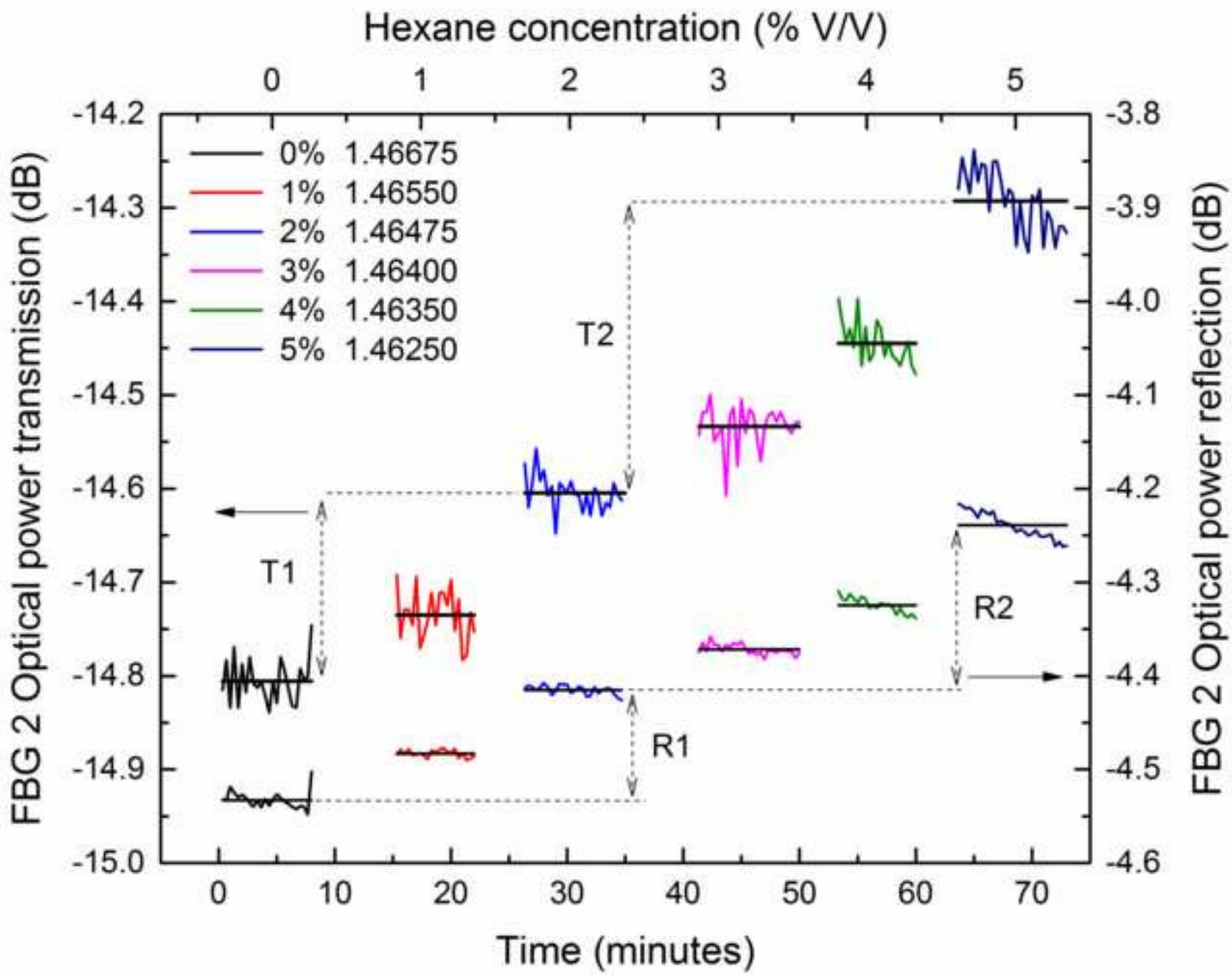
Hexane concentration (% V/V)
0
1
2
3
4
5
0% 1.46675
1% 1.46550
2% 1.46475
3% 1.46400
4% 1.46350
5% 1.46250
T1
T2
R1
R2
FBG 2 Optical power transmission (dB)
-14.2
-14.3
-14.4
-14.5
-14.6
-14.7
-14.8
-14.9
-15.0
FBG 2 Optical power reflection (dB)
-3.8
-3.9
-4.0
-4.1
-4.2
-4.3
-4.4
-4.5
-4.6
0
10
20
30
40
50
60
70
Time (minutes)